NeuroImage: Clinical 24 (2019) 102089

Contents lists available at ScienceDirect

NeuroImage: Clinical

journal homepage: www.elsevier.com/locate/ynicl

Widespread subcortical grey matter degeneration in primary lateral sclerosis: a multimodal imaging study with genetic profiling

Eoin Finegan[a], Stacey Li Hi Shing[a], Rangariroyashe H. Chipika[a], Mark A. Doherty[b], Jennifer C. Hengeveld[b], Alice Vajda[b], Colette Donaghy[c], Niall Pender[d], Russell L. McLaughlin[b], Orla Hardiman[a], Peter Bede[a,*]

[a] Computational Neuroimaging Group, Biomedical Sciences Institute, Trinity College Dublin, 152-160 Pearse Street, Dublin 2, Ireland
[b] Complex Trait Genomics Laboratory, Smurfit Institute of Genetics, Trinity College Dublin, Dublin, Trinity College Dublin, 152-160 Pearse Street, Dublin 2, Ireland
[c] Western Health & Social Care Trust, UK
[d] Department of Psychology, Beaumont Hospital Dublin, Ireland

ARTICLE INFO

Keywords:
Primary lateral sclerosis
neuroimaging
thalamus
basal ganglia
biomarkers
MRI

ABSTRACT

Background: Primary lateral sclerosis (PLS) is a low incidence motor neuron disease which carries a markedly better prognosis than amyotrophic lateral sclerosis (ALS). Despite sporadic reports of extra-motor symptoms, PLS is widely regarded as a pure upper motor neuron disorder. The post mortem literature of PLS is strikingly sparse and very little is known of subcortical grey matter pathology in this condition.

Methods: A prospective imaging study was undertaken with 33 PLS patients, 117 healthy controls and 100 ALS patients to specifically assess the integrity of subcortical grey matter structures and determine whether PLS and ALS have divergent thalamic, hippocampal and basal ganglia signatures. Volumetric, morphometric, segmentation and vertex-wise analyses were carried out in the three study groups to evaluate the integrity of thalamus, hippocampus, caudate, amygdala, pallidum, putamen and accumbens nucleus in each hemisphere. The hippocampus was further parcellated to characterise the involvement of specific subfields.

Results: Considerable thalamic, caudate, and hippocampal atrophy was detected in PLS based on both volumetric and vertex analyses. Significant volume reductions were also detected in the accumbens nuclei. Hippocampal atrophy in PLS was dominated by dentate gyrus, hippocampal tail and CA4 subfield volume reductions. The morphometric comparison of ALS and PLS cohorts revealed preferential medial bi-thalamic pathology in PLS compared to the predominant putaminal degeneration detected in ALS. Another distinguishing feature between ALS and PLS was the preferential atrophy of the amygdala in ALS.

Conclusions: PLS is associated with considerable subcortical grey matter degeneration and due to the extensive extra-motor involvement, it should no longer be regarded a pure upper motor neuron disorder. Given its unique pathological features and a clinical course which differs considerably from ALS, dedicated research studies and disease-specific therapeutic strategies are urgently required in PLS.

Glossary

ALS: Amyotrophic Lateral sclerosis, **ANCOVA**: Analysis of covariance, **BG**: Basal ganglia, **C9orf72**: chromosome 9 open reading frame 72, **CA**: Cornu ammonis, **FOV**: Field of view, **FWE**: Familywise error, **GC-ML-GD**: Molecular and granule cell layer of the dentate gyrus, **GM**: Grey matter, **HATA**: Hippocampal-amygdala transition area, **HC**: Healthy control, **HSP**: Hereditary Spastic Paraplegia, **IR-SPGR**: Inversion Recovery prepared Spoiled Gradient Recalled echo, **LMN**: Lower motor neuron, **M**: Mean, **MNI152**: Montreal Neurological Institute 152 standard space, **PBA**: Pseudobulbar affect, **PCL**: Pathological crying and laughing, **PLS**: Primary lateral sclerosis, **pTDP-43**: Phosphorylated 43kDa TAR DNA-binding protein, **SD**: Standard deviation, **T1 W**: T1-weighted imaging, **TE**: Echo time, **TFCE** – Threshold-free cluster enhancement, **TI**: Inversion time, **TIV**: Total intracranial volume, **TR**: Repetition time, **UMN**: Upper motor neuron

Introduction

Primary lateral sclerosis is an upper motor neuron predominant

* Corresponding Author. Tel: + 353 1 8964497
E-mail address: bedep@tcd.ie (P. Bede).

https://doi.org/10.1016/j.nicl.2019.102089
Received 29 July 2019; Received in revised form 2 October 2019; Accepted 9 November 2019
Available online 12 November 2019

motor neuron disease, with markedly slower progression rates and longer survival than ALS. (Floeter and Mills, 2009, Chipika et al., 2019) It has a number of distinguishing and overlapping features with ALS, but owing to its low incidence and paucity of post-mortem studies, relatively little is known of its patterns of cerebral disease burden. PLS is often regarded as a 'pure' upper motor neuron disorder and many of its cardinal clinical features; spasticity, gait impairment, dysarthria and pseudobulbar affect are solely attributed to upper motor neuron dysfunction. The dominance of widespread pyramidal signs renders the clinical detection of subtle cerebellar and extrapyramidal signs challenging. Existing imaging studies of PLS primarily focus on corticospinal tract, (Iwata et al., 2011, Müller et al., 2018)corpus callosum, (Unrath et al., 2010, Agosta et al., 2014) brainstem (Bede et al., 2019) and precentral gyrus (Butman and Floeter, 2007, Schuster et al., 2013) pathology and few studies have endeavoured to specifically characterise extra-motor involvement. With very few exceptions, (Clark et al., 2018, Finegan et al., 2019) most PLS studies describe similar imaging patterns to ALS. (Müller et al., 2018, Van Weehaeghe et al., 2016) The notion that PLS selectively affects the UMN system has led to the assumption that extra-motor manifestations, such as neuropsychological, cerebellar and extrapyramidal deficits are rare. However, recent reports of cognitive deficits, (de Vries et al., 2019) descriptions of widespread cerebellar degeneration (Finegan et al., 2019, Clark et al., 2017, Floeter et al., 2014) and the observation of considerable subcortical TDP-43 burden (Kosaka et al., 2012) have gradually challenged this perspective. Accordingly, the objective of this study is the comprehensive characterisation of subcortical grey matter involvement in PLS. An additional objective of this study is the identification of subcortical signatures that may distinguish PLS from ALS. Our hypothesis is that basal ganglia, hippocampal and thalamic pathology can be detected in PLS, and the subcortical signature of PLS is different from ALS.

Methods

Participants and ethics

Thirty-three PLS patients, 100 patients with ALS and 117 healthy controls (HC) were included in a prospective neuroimaging study. The clinical and demographic profiles of the study participants are summarised in Table 1. The study was approved by the Ethics (Medical Research) Committee – Beaumont Hospital, Dublin, Ireland, and all participants provided informed consent prior to inclusion. Participating ALS patients had 'probable' or 'definite' ALS according to the revised El Escorial research criteria (Brooks et al., 2000) and PLS patients were diagnosed according to the Gordon criteria. (Gordon et al., 2006) Inclusion criteria included the ability to lie supine in the scanner for the duration of data acquisition. Exclusion criteria included implanted medical devices, such as baclofen pumps or pacemakers which would have precluded MR imaging. ALS patients with comorbid frontotemporal dementia were not included. (Rascovsky et al., 2011) The healthy control cohort had no known neurological or psychiatric conditions, previous head injuries or established vascular risk factors.

Table. 1
The demographic and clinical profile of study participants.

	PLS n = 33	ALS n = 100	HC n = 117	p value
Gender (male)	19	(62)	56	0.11
Age-years (mean ± SD)	60.5 ± 10.5	59.8 ± 11.2	57.4 ± 11.9	0.19
Education-years (mean ± SD)	12.9 ± 3.4	13.5 ± 3.2	14.3 ± 3.3	0.04*
Handedness (right)	29	90	109	0.55
ALSFRS-r (mean ± SD)	34.4 ± 5.3	36.6 ± 7.5	N/A	0.11

Genetics

Whole exome sequencing was performed in 29 of the 33 PLS patients, as previously described. (Finegan et al., 2019) Briefly, sequence data were assessed for quality, aligned to the GRCh37 reference genome, annotated and analysed using cutadapt V.1.9.1 (Martin, 2011), SAMtools V1.7 (Li et al., 2009), Picard V.2.15.0, Plink V.1.9 (Purcell et al., 2007), R V.3.2.3, SnpEff V.4.3 (Cingolani et al., 2012) and Gemini V.0.20.1 (Paila et al., 2013). Samples were compared to 135 Irish controls sequenced as described previously. (Project Min, 2018, McLaughlin et al., 2015) Putative variants were defined as protein altering variants in the exons and splice sites of 33 genes linked to ALS on the ALS online database (Abel et al., 2013) and 70 genes linked to HSP in the literature. (Klebe et al., 2015) The presence of the *C9orf72* hexanucleotide repeat expansion was determined using repeat-primed polymerase chain reaction (PCR) as described previously (Byrne et al., 2012). Of the 100 ALS patients enrolled in neuroimaging, whole-genome sequence data was available for 44 patients (Project Min, 2018) and targeted DNA sequence data for a further 27. (Kenna et al., 2013) Patients were screened for previously reported ALS variants. *C9orf72* repeat expansion status was determined in 97 patients. (Byrne et al., 2012)

Magnetic resonance imaging

Magnetic Resonance Imaging was performed on a 3 Tesla Philips Achieva system using an 8-channel receive-only head coil. T1-weighted images were acquired using a 3 D Inversion Recovery prepared Spoiled Gradient Recalled echo (IR-SPGR) sequence; FOV: 256 × 256 × 160 mm, spatial resolution: 1 × 1 × 1 mm, TR/TE = 8.5/3.9 ms, TI = 1060 ms, flip angle = 8°, SENSE factor = 1.5 acquisition time = 7 min 30 s. A multimodal approach was implemented to comprehensively characterise the subcortical grey matter profile of the three study groups. First, total intracranial volumes (TIV) were calculated and the volumes of individual subcortical grey matter structures estimated. Subsequently, hippocampal segmentation was performed to estimate the volumes of specific subfields. Finally, morphometric analyses were carried out to identify focal pathological changes and vertex analyses were undertaken to characterise patterns of shape deformations.

Volumetric analyses

Total intracranial volume (TIV) was estimated for each participant to be used as a covariate for volumetric analyses. The FSL imaging suite was utilised for TIV estimations which were performed by linearly aligning each subject's skull-stripped brain to the standard MNI152 brain image in MNI space, calculating the inverse of the determinant of the affine registration matrix and multiplying it by the size of the template. Registration to template was undertaken using FSL-FLIRT, (Jenkinson and Smith, 2001) and FSL-FAST was used for tissue type segmentation. (Zhang et al., 2001) Subsequent to brain extraction with FSL-BET, the subcortical segmentation and registration tool FIRST (Patenaude et al., 2011) of the FMRIB's Software Library (FSL) was used to estimate the volumes of subcortical grey matter structures in the left and right hemispheres separately; the hippocampus, amygdala, thalamus, nucleus accumbens, caudate nucleus, putamen, and pallidum. Pipelines for subcortical segmentation and volume estimations were previously described. (Bede et al., 2013, Bede et al., 2018) Briefly, FSL-FIRST uses a two-stage affine registration procedure to register input T1 data sets to the Montreal Neurological Institute 152 (MNI152) standard space and a model-based approach is then implemented for the segmentation of subcortical structures. The accuracy of subcortical segmentation was individually verified for all participants. Subcortical mesh and volumetric outputs are generated following automatic boundary corrections. Analyses of covariance (ANCOVA) were

conducted to compare volumes of subcortical structures between study groups. Assumptions of normality, linearity and homogeneity of variances were verified. Volumes of subcortical grey matter structures were included as dependent variables, and study group allocation as the categorical independent variable. Age, education, gender and TIV were used as covariates and the ALS versus PLS contrasts were additionally corrected for symptom duration. A p-value ≤ 0.05 was considered significant. A table was generated with the estimated marginal means of volumes for each anatomical structure, standard error, between-group ANCOVA significance and p-values for Bonferroni-corrected post hoc testing. For illustrative purposes, estimated marginal means of volumes were plotted with confidence intervals to highlight group-specific volumetric traits for each structure. To illustrate the comparative subcortical profiles of PLS and ALS, percentage volume reductions were also calculated based on estimated marginal means for each structure with reference to healthy controls and plotted on a radar (spider) chart.

Hippocampal subfields

Version 6.0 of the FreeSurfer image analysis suite was used for the segmentation of the hippocampus into cytologically-defined subfields. (Fischl, 2012) T1-weighted data pre-processing included the removal of non-brain tissues, segmentation of the subcortical white matter and deep grey matter structures, intensity normalization, tessellation of the grey matter-white matter boundaries, and automated topology correction. The hippocampus was subsequently segmented into the following subfields using the hippocampal stream of the FreeSurfer package: CA1, CA2/3, CA4, fimbria, subiculum, hippocampal tail, molecular layer, molecular and granule cell layer of the dentate gyrus (GC-ML-DG), and hippocampal-amygdala transition area (HATA) (Iglesias et al., 2015, Christidi et al., 2019). Figure 1. To illustrate the comparative hippocampal profiles of PLS and ALS, percentage volume reductions were calculated based on estimated marginal means for each subfield with reference to controls and plotted on a radar (spider) chart.

Vertex analyses

As volumetric analyses only capture overall atrophy considering the entire structure, additional shape (vertex) and morphometric analyses were carried out to characterise deformation patterns and focal density reductions within the subcortical grey matter structures. Vertex-wise statistics were performed using FMRIB's subcortical segmentation and registration tool FIRST. Vertex locations of individual study participants were projected on the surface of an average template shape as scalar values, positive values representing vertex locations outside the surface and negative values inside. Intergroup differences were explored using permutation-based non-parametric testing as implemented in FSL Randomise. (Winkler et al., 2014) Design matrices for the comparison of PLS patient with healthy controls included age, gender, TIV and education. The design matrix comparing the subcortical deformation profile of PLS and ALS patients included age, gender, TIV, education and symptom duration. The threshold-free cluster enhancement (TFCE) method (Smith and Nichols, 2009) was used and results were corrected for multiple comparisons across space (FWE < 0.05).

Morphometry

Following brain extraction and tissue-type segmentation, grey-matter partial volume images were aligned to MNI152 standard space using affine registration. Brain removal and tissue-type segmentation outcomes were individually verified. A study specific template was created, to which the grey matter images from each subject were non-linearly coregistered. A voxelwise generalized linear model and permutation-based non-parametric testing was used to highlight density alterations in a merged basal ganglia grey matter mask. (Winkler et al., 2014, Nichols and Holmes, 2002) The Harvard-Oxford subcortical probabilistic structural atlas was used to generate a merged basal ganglia mask incorporating the bilateral caudate, thalamus, accumbens, hippocampus, amygdala, putamen, and pallidum. (Frazier et al., 2005, Desikan et al., 2006)

Results

Subcortical grey matter atrophy

Subcortical segmentation confirmed statistically significant volume reductions in PLS compared to healthy controls in the following structures: left thalamus, right thalamus, left hippocampus and a trend

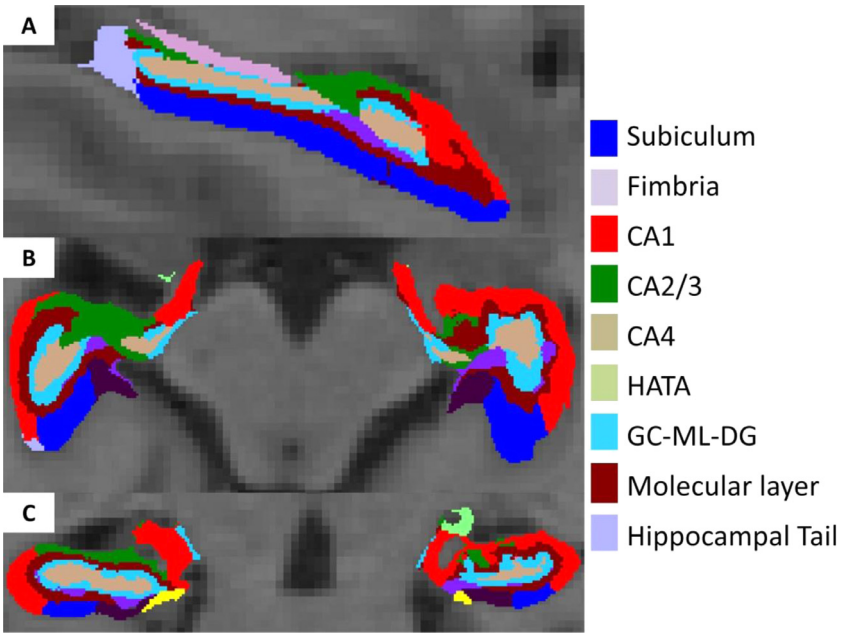

Figure. 1. Hippocampal segmentation and subfields. CA: cornu ammonis, HATA: hippocampal-amygdala transition area, GC-ML-GD- molecular and granule cell layer of the dentate gyrus

Table. 2
Subcortical grey matter volumes (mm3) in healthy controls (HC), ALS patients (ALS) and PLS patients (PLS). Estimated marginal means and standard error are adjusted for age, gender, education and total intracranial volume (TIV) (Age = 58.77, Gender = 1.45, Edu = 13.78, TIV = 1429699.38) *Significant intergroup differences are flagged with asterisks. a The ALS vs PLS post-hoc comparisons are adjusted for age, gender, education, TIV and symptom duration (age = 59.99, Gender = 1.39, Edu = 13.31,TIV = 1440387.86, Symptom Duration(m) = 45.71. t indicates a statistical trend

Structure	Study group	Estimated marginal mean	Standard error	ANCOVA *p* value	ALS vs HC	PLS vs HC	ALS vs PLS[a]
left Thalamus	HC	7614.0	52.4	<.001*	.007*	<.001*	1.0
	ALS	7376.1	56.3				
	PLS	7044.0	97.9				
Right Thalamus	HC	7402.8	48.9	<.001*	.008*	<.001*	1.0
	ALS	7182.0	52.6				
	PLS	6896.5	91.5				
Left Caudate	HC	3409.6	32.1	.023*	.032*	.120	.168
	ALS	3287.5	34.5				
	PLS	3283.3	60.0				
Right Caudate	HC	3576.6	35.5	.080	.554	.093	1.0
	ALS	3506.8	38.1				
	PLS	3412.4	66.3				
Left Putamen	HC	4692.2	44.0	.267	.821	.400	1.0
	ALS	4620.7	47.3				
	PLS	4550.8	82.3				
Right Putamen	HC	4741.9	46.3	.414	.975	.724	1.0
	ALS	4674.1	49.8				
	PLS	4625.6	86.7				
Left Pallidum	HC	1773.1	19.4	.575	1.0	1.0	.021
	ALS	1751.6	20.8				
	PLS	1733.7	36.3				
Right Pallidum	HC	1779.5	21.7	.340	1.0	.469	.378
	ALS	1775.4	23.3				
	PLS	1713.7	40.5				
Left Hippocampus	HC	3805.1	45.1	.007*	.022*	.042*	.425
	ALS	3624.1	48.5				
	PLS	3566.6	84.4				
Right Hippocampus	HC	3888.5	45.7	.046*	.085	.194	1.0
	ALS	3739.1	49.1				
	PLS	3707.4	85.4				
Left Amygdala	HC	1213.9	22.7	.027*	.024*	1.0	1.0
	ALS	1124.0	24.4				
	PLS	1189.4	42.4				
Right Amygdala	HC	1178.8	23.5	.155	.162	1.0	.141
	ALS	1111.2	25.3				
	PLS	1144.2	44.0				
Left Accumbens	HC	493.8	10.5	.190	.217	1.0	.019*
	ALS	465.8	11.3				
	PLS	473.8	19.6				
Right Accumbens	HC	378.2	10.2	.012*	.033*	.057	.550
	ALS	339.6	10.9				
	PLS	326.9	19.0				

of right accumbens atrophy (p = 0.056) accounting for age, gender, TIV and education. These structures also exhibited atrophy in the ALS group compared to controls, and significant additional volume reductions were noted in the left amygdala, left caudate and right accumbens. Table 2. The comparison of the two patient cohorts confirmed disproportionate left pallidum and left accumbens atrophy in ALS. The volumes of other subcortical structures were not significantly different between the patient groups. Based on percentage volume reductions, the most affected structure in PLS was the accumbens nucleus followed by the thalamus, hippocampus and caudate. Figure 2. This was different from ALS where the second most affected structure was the amygdala.

Hippocampal subfield profiles

The evaluation of hippocampal subfields in PLS revealed focal atrophy in the dentate (GC-ML-DG), molecular layer, and CA4 subfields compared to controls as well as a statistical trend for volume reductions in CA1 and CA2/3. Figure 3. This pattern of selective subfield vulnerability was similar to that observed in ALS, with the exception that HATA volumes were significantly reduced in ALS which was not the case in PLS. Table 3. No significant volume reductions were identified in the hippocampal tail, subiculum, or fimbria in either patient group compared to controls. Moreover, no hippocampal segments were significantly different between ALS and PLS.

Vertex analyses

Shape analyses revealed statistically significant vertex deformations in PLS compared to controls in the bilateral thalami, hippocampi and caudate nuclei. Figure 4. Patterns of surface-projected atrophy were strikingly symmetric in the two hemispheres. Preferential lateral hippocampal shape deformation and predominantly medial thalamic atrophy was observed. Most of the medial aspect of the body of the caudate nucleus, a small region of the lateral body of the caudate and the lateral- inferior aspect of the head of the left caudate was also affected in PLS. Vertex changes in the pallidum, and putamen did not reach significance compared to controls. The vertex-wise comparison of the ALS and PLS cohorts only reached significance in the left pallidum revealing atrophy in the superior and inferior aspect of the structure in the PLS cohort compared to ALS. Figure 5.

Focal morphometric alterations

The morphometric analyses restricted to the subcortical grey matter mask revealed left putamen and left pallidum pathology in PLS compared to controls at p < 0.05 TFCE FWE. Figure 6. This pattern is

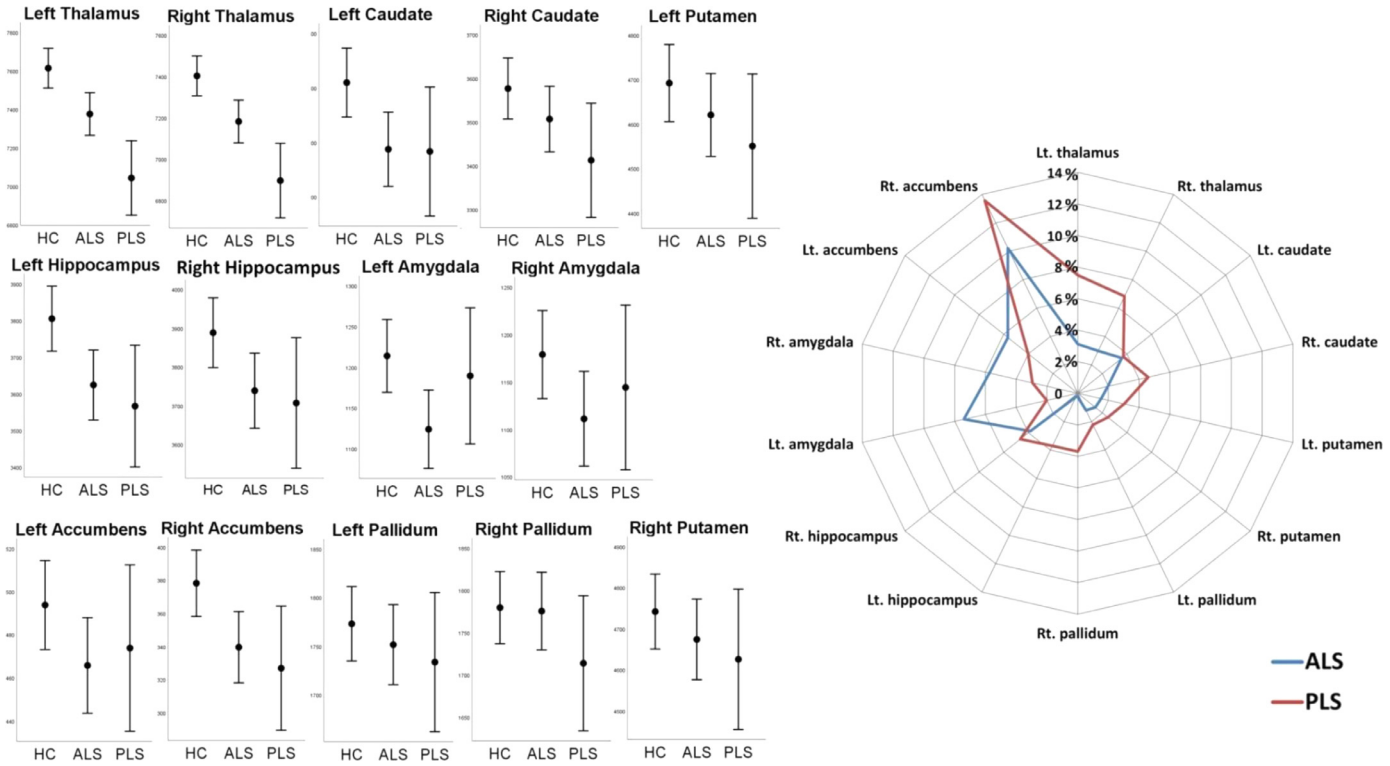

Figure. 2. Left: The volumetric profile of subcortical grey matter structures in PLS, ALS and healthy controls (HC) based on estimated marginal means adjusted for age, gender, total intracranial volume (TIV) and education. Error bars represent 95% confidence intervals. Right: the comparative volumetric profile of subfields based on percentage reduction with reference to controls.

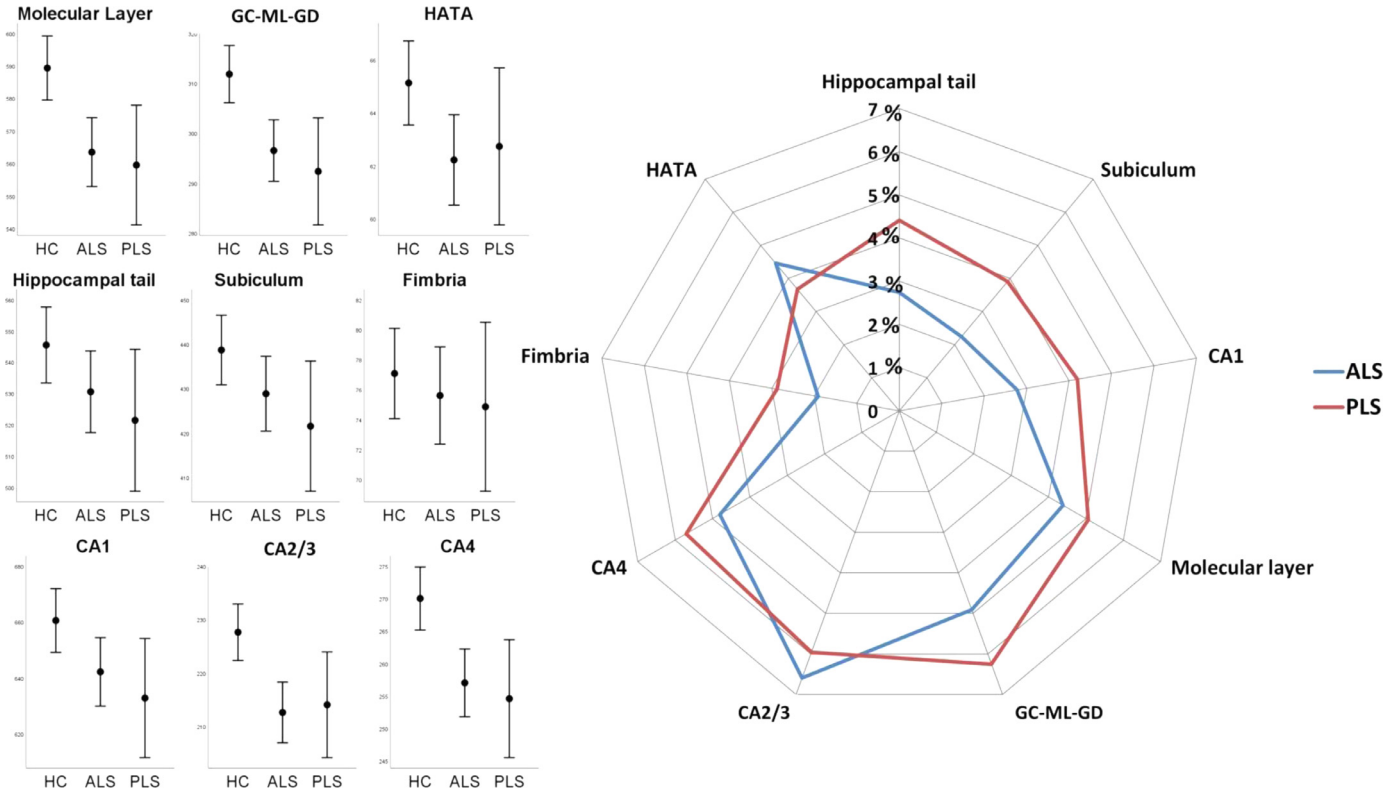

Figure. 3. Left: The volumetric profile of hippocampal subfield in PLS, ALS and healthy controls (HC) based on estimated marginal means adjusted for age, gender, total intracranial volumes (TIV) and education. Error bars represent 95% confidence intervals. Right: the comparative volumetric profile of subfields based on percentage change with reference to controls. CA: cornu ammonis, HATA: hippocampal-amygdala transition area, GC-ML-GD- molecular and granule cell layer of the dentate gyrus

Table. 3
Hippocampal subfield volumes (mm^3) in healthy controls (HC), ALS patients (ALS) and PLS patients (PLS) Estimated marginal means and standard error are adjusted for age, gender, education and total intracranial volume (TIV) Age = 58.77, Gender = 1.45, Edu = 13.78, TIV = 1429699.38. *Significant intergroup differences are flagged with asterisks. [a] The ALS vs PLS post-hoc comparisons are adjusted for age, gender, education, TIV and symptom duration(age = 59.99, Gender = 1.39, Edu = 13.31,TIV = 1440387.86, Symptom Duration(m) = 45.71). [t] indicates statistical trends CA: cornu ammonis, HATA: hippocampal-amygdala transition area, GC-ML-GD- molecular and granule cell layer of the dentate gyrus

Structure	Study group	Estimated marginal mean- mm^3	Standard error	ANCOVA *p* value	ALS vs HC	PLS vs HC	ALS vs PLS[a]
Hippocampal Tail	HC	545.5	6.2	.107	.310	.206	1.0
	ALS	530.6	6.6				
	PLS	521.5	11.5				
Subiculum	HC	438.7	4.0	.077	.289	.133	1.0
	ALS	428.9	4.3				
	PLS	421.6	7.4				
CA1	HC	660.5	5.8	.029*	.099	.077	1.0
	ALS	642.2	6.2				
	PLS	632.9	10.8				
Molecular Layer	HC	589.4	5.0	<.001*	.002*	.017*	1.0
	ALS	563.5	5.4				
	PLS	559.5	9.3				
GC-ML-GD	HC	311.8	2.9	<.001*	.001*	.006*	.755
	ALS	296.5	3.1				
	PLS	292.3	5.4				
CA2/3	HC	227.6	2.7	<.001*	<.001*	.056	1.0
	ALS	212.6	2.9				
	PLS	214.1	5.0				
CA4	HC	270.0	2.5	<.001*	.001*	.011*	.772
	ALS	257.0	2.6				
	PLS	254.6	4.6				
Fimbria	HC	77.1	1.5	.720	1.0	1.0	1.0
	ALS	75.6	1.6				
	PLS	74.9	2.9				
HATA	HC	65.1	0.8	.045*	.047*	.494	1.0
	ALS	62.2	0.9				
	PLS	62.7	1.5				

distinctly different from the right hippocampal and amygdala atrophy observed in ALS compared to controls. The direct comparison of ALS and PLS cohorts, revealed medial bi-thalamic atrophy in PLS compared to ALS and right putaminal changes in ALS compared to PLS. Figure 7.

Clinical and genetic profiling

Thirty-two of the 33 PLS patients had lower limb symptom onset. Ninety-one percent (n = 30) of the patients used a walking aid for safe ambulation and 79% (n = 26) experienced at least one fall during the 12-months preceding their MRI scan. The functional profile of the group based on ALSFRS-r demonstrated lower limb symptom predominance in the entire cohort: total ALSFRS-r M = 34.4, SD 5.3; bulbar sub-score M = 9.2, SD = 2.1; upper-limb sub-score M = 8.6, SD 2.1; lower limb sub-score ALSFRS-r sub-score M = 5.4, SD 1.6; respiratory sub-score M = 11.1, SD = 1.4. The Penn UMN score (Woo

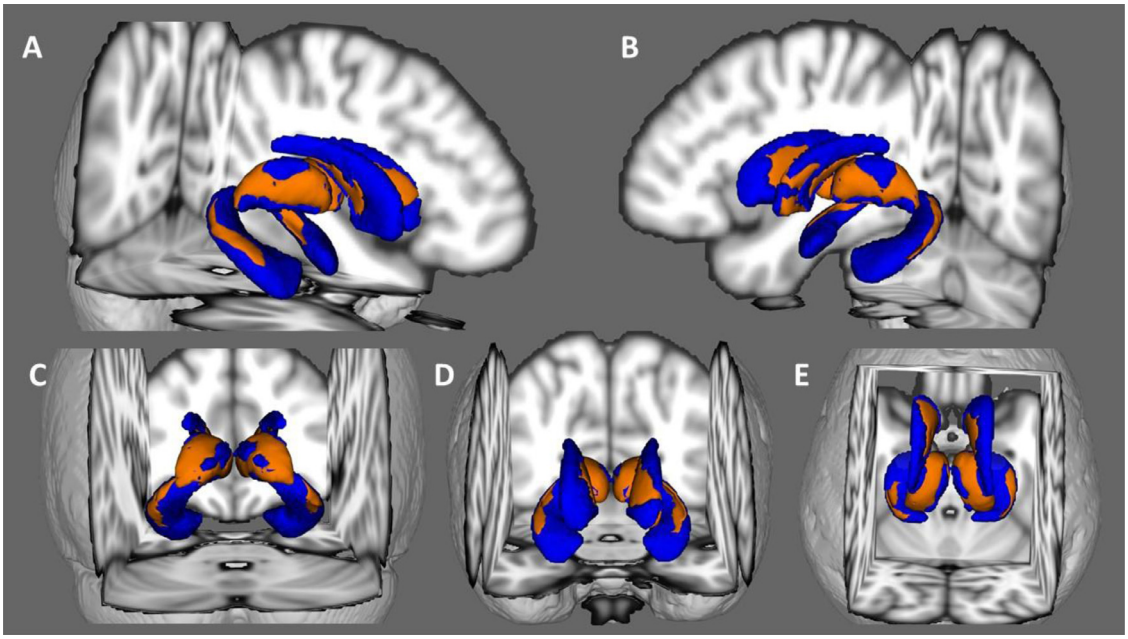

Figure. 4. Subcortical shape alterations in PLS compared to controls. Surface projected patterns of atrophy are shown in orange over the 3-dimensional mesh representation of the thalami, caudate, and hippocampi shown in blue. $p < 0.05$ FWE.

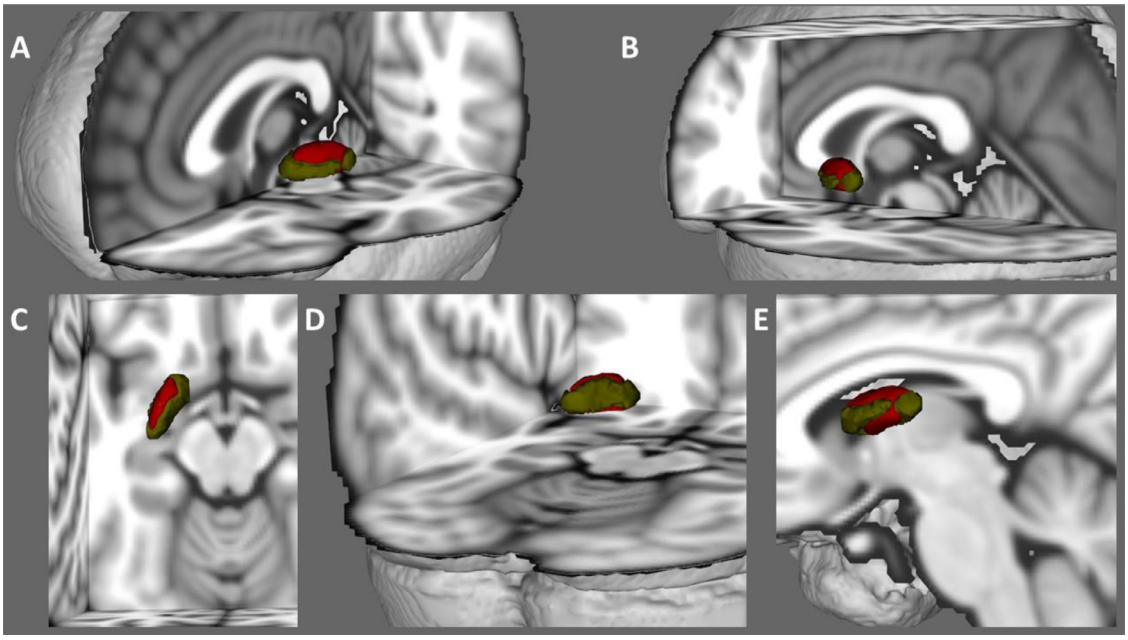

Figure. 5. Subcortical shape alterations in PLS compared to ALS. Surface projected patterns of atrophy are shown in red over the 3-dimensional mesh representation of the left pallidum shown in green. $p < 0.05$ FWE.

et al., 2014) profile was also consistent with selective functional impairment (higher scores indicate greater burden): total score (max = 32) M = 20.3, SD = 6.3; bulbar score (max = 4) M = 1.8, SD 1,4; upper limb score (max = 14) M = 8.6, SD 3.4; lower limb score (max = 14) M = 9.8, SD = 2.5. Finger-tapping rates were: right hand M = 2.59/s, SD = 1.32; left hand M = 2.34/s, SD = 1.12; right foot M = 1.41/s, SD 0.69; left foot M = 1.36/s, SD 0.78. Genetic testing data were available on 29 PLS patients. No PLS patient carried the

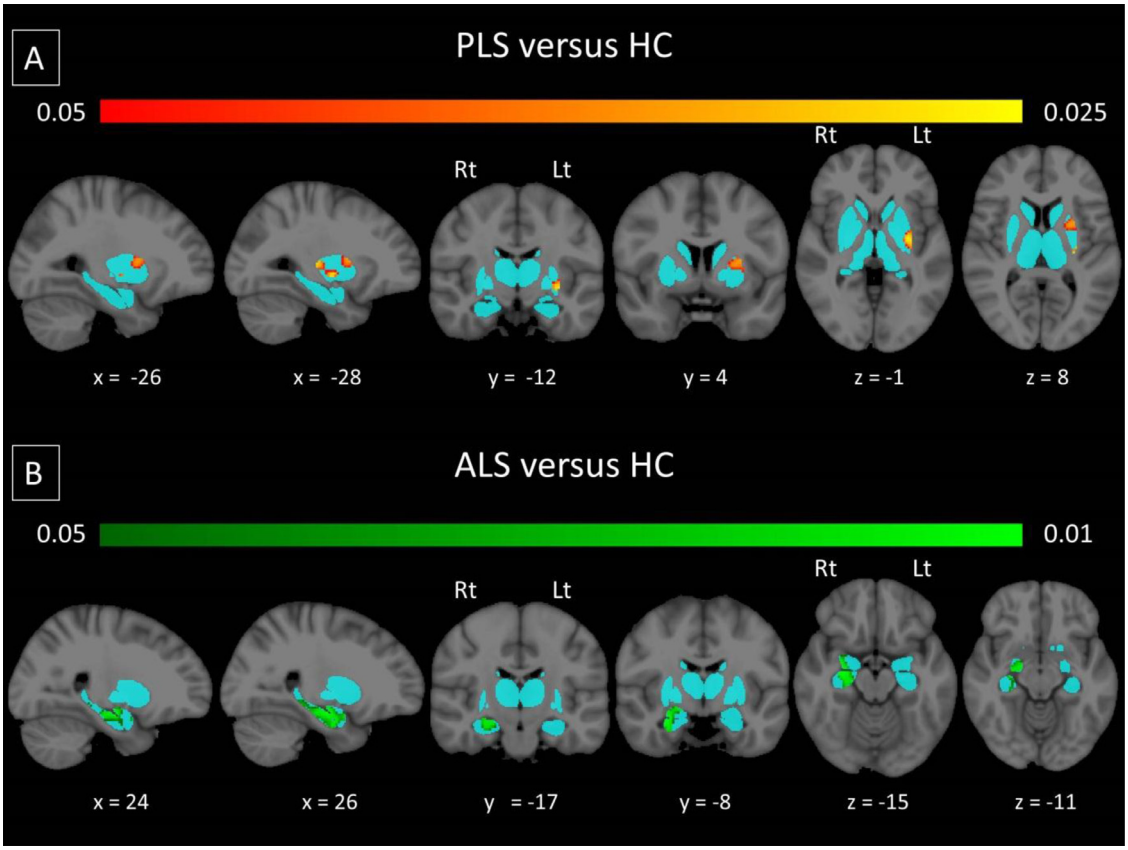

Figure. 6. Morphometric changes in PLS (top) and ALS (bottom) with reference to healthy controls in a subcortical grey matter mask (light blue). Radiological convention is used and MNI coordinates are provided. $p < 0.05$ TFCE FWE corrected for age, gender, total intracranial volume and education. Radiological convention is used; Rt – right, Lt – Left

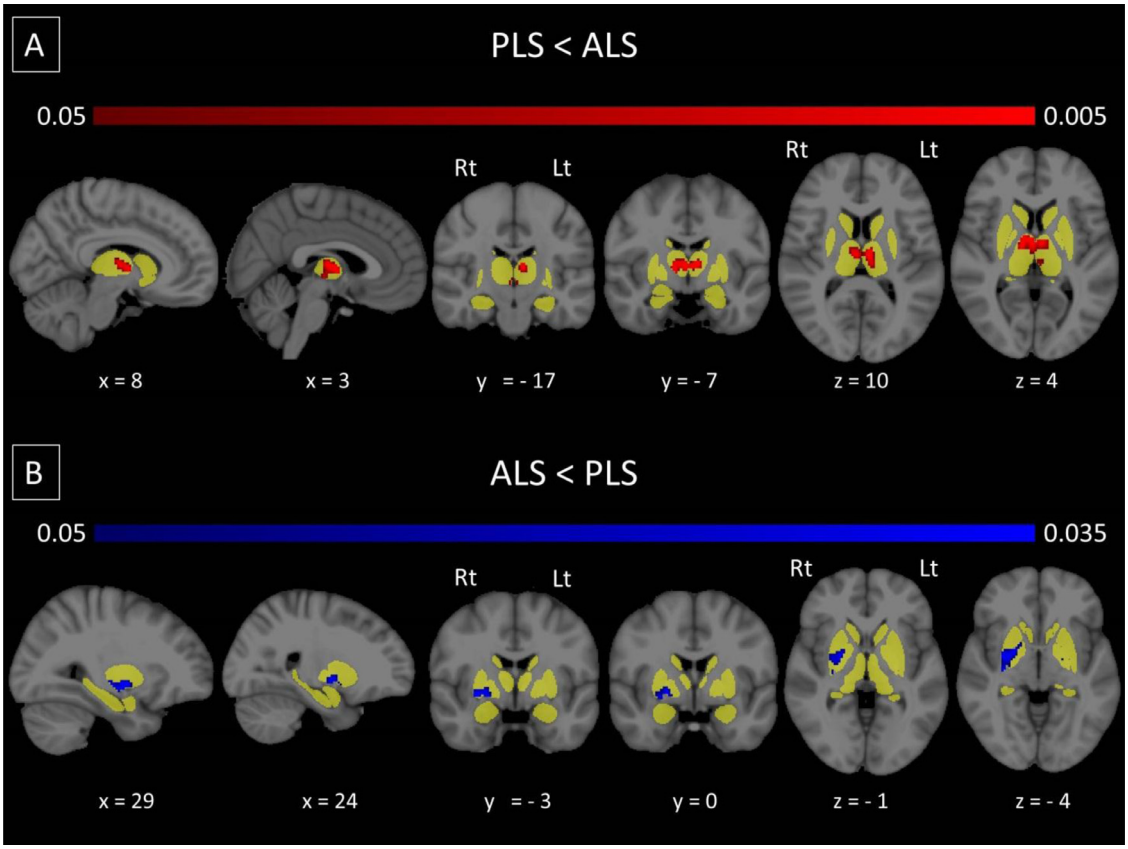

Figure. 7. Patterns of subcortical grey matter alterations in PLS compared to ALS (top) and in ALS compared to PLS (bottom) in a subcortical grey matter mask (yellow). Radiological convention is used and MNI coordinates are provided. $p < 0.05$ TFCE FWE corrected for age, gender, TIV, symptom duration and education. Radiological convention is used; Rt – right, Lt – Left

c9orf72 hexanucleotide expansion and no PLS patients carried mutations previously implicated in ALS or HSP. Eleven of 100 ALS patients carried the C9orf72 repeat expansion.

Discussion

Our finding of considerable subcortical grey matter degeneration in PLS is consistent with emerging reports of subcortical pTDP-43 burden, and extra-motor clinical deficits. The importance of characterising extra-motor pathology in PLS is twofold; academic and clinical. From an academic perspective it provides compelling evidence that PLS is not a "pure" UMN disorder, and that the underlying pathology is not confined to the motor cortices and corticospinal tracts. While mechanisms of propagation in PLS remain elusive, it seems that progressive pathological changes take place in PLS, both spatially and chronologically. In ALS, a number of spreading mechanisms have been proposed; including prion-like propagation, progressive changes mediated by inflammation, impaired inhibitory function, hypermetabolic changes, none of which has been specifically studied in PLS. (Chipika et al., 2019, Schuster et al., 2015) In ALS, pathological staging systems have been developed based on TDP-43 disease burden, (Brettschneider et al., 2013) and attempted in vivo validations published based on imaging data, (Kassubek et al., 2014) but these have not been applied to PLS to date. (Brettschneider et al., 2013, Kassubek et al., 2014, Geser et al., 2011, Bede, 2019)

From a clinical perspective, the literature on cognitive and behavioural impairment in PLS is sparse and the suggestion that cognitive impairment might be present in a high proportion of PLS patients is relatively novel. (de Vries et al., 2019, de Vries et al., 2017) However, there is now a growing recognition that similarly to ALS, (Phukan et al., 2012, Elamin et al., 2011, Burke et al., 2016, Elamin et al., 2017) widespread deficits in social cognition, verbal fluency, executive function and memory impairment can also be detected in PLS. (de Vries et al., 2019) In our cohort of patients language deficits were present in 24%, verbal fluency was abnormal in 18% and 12% had abnormal memory performance on ECAS. (Abrahams et al., 2014) Given the high prevalence of verbal fluency deficits in the PLS group, it is noteworthy that significant bilateral thalamic morphological changes have previously been described in non-fluent variant primary progressive aphasia and significant hippocampal atrophy has been associated with behavioural-variant FTD; (Bede et al., 2018, Omer et al., 2017) observations which are consistent with our current findings. As in ALS, (Elamin et al., 2017) behavioural manifestations are not uncommon in PLS, which typically include loss of sympathy, apathy, as well as disinhibition. There has been also been reports of personality changes in PLS, such as late-onset obsessive compulsive disorder. (Bersano et al., 2018) Studies from other motor neuron diseases suggest that the basal ganglia may play a role in compensatory processes (Abidi et al., 2019) and their degeneration may contribute bulbar dysfunction. (Yunusova et al., 2019)

Similar to ALS, (Feron et al., 2018) extrapyramidal dysfunction has been previously reported in PLS, including freezing and postural instability (Mabuchi et al., 2004) which is sometimes referred to as "PLS-plus." (Rowland, 2005) PLS cases were reported which initially presented with frank parkinsonism. (Gordon et al., 2006) However, the detection of extrapyramidal signs in the presence of widespread UMN degeneration is challenging based on clinical assessment alone, and may require computational gait analyses. (Feron et al., 2018) It is conceivable that extrapyramidal deficits contribute to gait impairment and fall risk in many patients with PLS. Based on anecdotal functional improvement on levodopa, a small clinical trial is currently underway to evaluate its use in PLS and ALS. (Clinicaltrials.gov 2019)

In addition to the neuropsychological and extrapyramidal manifestations of subcortical degeneration in PLS, it is likely that basal ganglia pathology also contributes to pseudobulbar affect (PBA). (Christidi et al., 2018, Bede and Finegan, 2018, Finegan et al., 2019) PBA is a very common symptom of PLS, (Thakore and Pioro, 2014) and in our cohort with 15 of 33 (45%) of PLS patients were affected. While PBA is classically linked to corticobulbar tract degeneration, it is increasingly clear that cerebellar and basal ganglia pathology also contribute to the aetiology of PBA. (Floeter et al., 2014, Bede and Finegan, 2018, Finegan et al., 2019) PBA has been previously linked to imaging changes in the putamen in ALS (Christidi et al., 2017), and basal ganglia pathology in stroke and MS. (Ghaffar et al., 2008) The clinical relevance of extra-motor changes in PLS is particularly important as this motor neuron disease phenotype carries a relatively good prognosis compared to ALS (Finegan et al., 2019) and extrapyramidal and neuropsychological impairment may impact on financial decisions, participation in clinical trials, driving, compliance with assistive devices, fall risk and impact on caregiver burden. (Olney et al., 2005, Elamin et al., 2013, Christidi et al., 2018)

While hippocampal degeneration is a recognised feature of ALS, (Machts et al., 2015, Christidi et al., 2018) it has not been specifically studied in PLS to date. Our volumetric analyses have captured overall hippocampal atrophy, and the parcellation of the structure revealed selective subfield vulnerability. The dentate (GC-ML-DG), molecular layer, and CA1, CA2/3 and CA4 subfields were preferentially affected with the relative sparing of the hippocampal tail, subiculum, and fimbria. The characterisation of affected and unaffected regions in PLS may have implications for the development of classification algorithms. (Bede et al., 2016, Grollemund et al., 2019) Two subcortical regions were identified where significant degeneration occurs in ALS, but not in PLS; the left amygdala and HATA. The majority of imaging studies in PLS describe imaging features similar to ALS. (Finegan et al., 2019, Schuster et al., 2016, Bede et al., 2018) The identification of PLS-specific imaging signatures which are distinct from ALS are clinically relevant, as they may contribute to the development of diagnostic applications for suspected PLS cases which don't meet the current 4-year symptom duration criterion for diagnosis. (Clark et al., 2018, Schuster et al., 2017) Disease-specific imaging features are increasingly utilised in complex classification algorithms to provide a diagnostic probability, (Grollemund et al., 2019, Bede et al., 2017, Querin et al., 2018, Schuster et al., 2016) or to model prognostic outcomes. (Schuster et al., 2017)

Our finding of extensive subcortical degeneration in PLS is consistent with previous pathology reports. A post-mortem study on an individual with PLS reported marked atrophy of the thalamus and striatum. (Sugihara et al., 1999) Another study detected considerable caudate atrophy and identified TDP-43 burden in this structure. While there is a striking paucity of post-mortem PLS studies, TDP-43 inclusions have been described in the striatum, amygdala and hippocampus. (Kosaka et al., 2012) Other sporadic reports exist of TDP-43 burden the dentate gyrus and amygdala. (Fu et al., 2010) A recent post-mortem study of PLS identified significant basal ganglia involvement keeping with the extra-pyramidal signs recorded ante-mortem. (Hirsch-Reinshagen et al., 2019) Consistent with our imaging findings, hippocampal TDP-43 inclusions were also evident, specifically involving the dentate gyrus and cornu ammonis (CA).

Extra-motor involvement in ALS, (Christidi et al., 2018) particularly extensive temporal lobe and anterior frontal pathology, is often associated with *C9orf72* hexanucleotide expansions. (Bede et al., 2013, Christidi et al., 2018) It is noteworthy that in our cohort of PLS patients, none of the study participants carried the pathological hexanucleotide expansion demonstrating that hippocampal and accumbens pathology cannot be solely attributed to *C9orf72* mutations.

This study is not without limitations. Owing to the low incidence of PLS the sample size of our cohort is limited despite population-based recruitment efforts. Our study has a cross-sectional design which precludes the longitudinal assessment of subcortical changes in this cohort. As with previous comparative studies of PLS and ALS, PLS subjects in our cohort had substantially longer symptom duration than the ALS group. Furthermore, the PLS group and the healthy controls were not matched for education. Accordingly, both symptom duration and years of education were included as covariates in the statistical models, in addition to demographic factors. (Bede et al., 2013) An additional limitation of our study is the lack of post mortem data which would be instrumental in validating our imaging findings. As current diagnostic criteria require a symptom duration of four years, it is unclear whether the subcortical changes described herein are a late or early features of PLS. Very few longitudinal studies exist in PLS. Innovative studies of suspected PLS patients, or 'pre-PLS' cohorts have been previously undertaken to describe early imaging features. (Clark et al., 2018) Longitudinal studies in ALS indicate early ceiling effects in white matter metrics, which capture considerable integrity changes at baseline with limited progression over time. Grey matter metrics in ALS however show continued decline in the later stages of the disease making them superior monitoring marker candidates. (Westeneng et al., 2015, Bede and Hardiman, 2018) These observations provide the rationale to undertake longitudinal PLS studies focusing on both cortical and subcortical grey matter metrics.

Conclusions

PLS should no longer be regarded as a pure upper motor neuron disorder, as it is associated with marked thalamic, hippocampal and basal ganglia atrophy. The severity of subcortical grey matter degeneration observed in PLS is comparable to ALS, but the anatomical patterns are different. These data demonstrate that PLS exhibits a number of unique features that underpin a clinical course which is markedly distinct from ALS. In the era of precision medicine, PLS urgently needs dedicated imaging studies, disease-specific clinical trials, and staging systems to develop effective disease modifying strategies

Declaration of Competing Interest

Peter Bede is the patron of the Irish motor neuron disease association (IMNDA), the head of the computational neuroimaging group (CNG) in Trinity College Dublin, member of the steering committee of the Neuroimaging Society of ALS (NiSALS) and member of the biomedical research advisory panel of the UK MND association (MNDA). These affiliations had no impact on the opinions expressed herein.

Acknowledgements

The authors are thankful for the kindness and generosity of all patients, their families and the healthy controls for participating in this research project. Without their support, this project would not have been possible. Peter Bede and the computational neuroimaging group is supported by the Health Research Board (HRB – Ireland; HRB EIA-2017-019), the Andrew Lydon scholarship, the Irish Institute of Clinical Neuroscience IICN – Novartis Ireland Research Grant, the Iris O'Brien Foundation, the Research Motor Neuron (RMN-Ireland) Foundation and the Irish Motor Neuron Disease Association (IMNDA). Russell L McLaughlin is supported by the Motor Neurone Disease Association (957-799) and Science Foundation Ireland (17/CDA/4737). Mark A Doherty is supported by Science Foundation Ireland (15/SPP/3244). The sponsors of this study had no role in the design, analyses, presentation of this work or the decision to submit these findings for publication.

Supplementary materials

Supplementary material associated with this article can be found, in the online version, at doi:10.1016/j.nicl.2019.102089.

References

Abel, O, Shatunov, A, Jones, AR, Andersen, PM, Powell, JF, Al-Chalabi, A, 2013. Development of a Smartphone App for a Genetics Website: The Amyotrophic Lateral Sclerosis Online Genetics Database (ALSoD). JMIR mHealth and uHealth 1 e18-e18.

Abidi, M, de Marco, G, Couillandre, A, Feron, M, Mseddi, E, Termoz, N, Querin, G, Pradat, PF, Bede, P, 2019. Adaptive functional reorganization in amyotrophic lateral sclerosis: coexisting degenerative and compensatory changes. Eur J Neurol.

Abrahams, S, Newton, J, Niven, E, Foley, J, Bak, TH, 2014. Screening for cognition and behaviour changes in ALS. Amyotrophic lateral sclerosis & frontotemporal degeneration 15, 9–14.

Agosta, F, Galantucci, S, Riva, N, Chio, A, Messina, S, Iannaccone, S, Calvo, A, Silani, V, Copetti, M, Falini, A, Comi, G, Filippi, M, 2014. Intrahemispheric and interhemispheric structural network abnormalities in PLS and ALS. Hum Brain Mapp 35, 1710–1722.

Bede, P, 2019. The histological correlates of imaging metrics: postmortem validation of in vivo findings. Amyotrophic lateral sclerosis & frontotemporal degeneration 1–4.

Bede, P., et al., 2019. Brainstem pathology in amyotrophic lateral sclerosis and primary lateral sclerosis: A longitudinal neuroimaging study. Neuroimage: Clinical.

Bede, P, Elamin, M, Byrne, S, Hardiman, O, 2013. Sexual dimorphism in ALS: Exploring gender-specific neuroimaging signatures. Amyotrophic lateral sclerosis & frontotemporal degeneration.

Bede, P, Elamin, M, Byrne, S, McLaughlin, RL, Kenna, K, Vajda, A, Pender, N, Bradley, DG, Hardiman, O, 2013. Basal ganglia involvement in amyotrophic lateral sclerosis. Neurology 81, 2107–2115.

Bede, P, Finegan, E, 2018. Revisiting the pathoanatomy of pseudobulbar affect: mechanisms beyond corticobulbar dysfunction. Amyotrophic lateral sclerosis & frontotemporal degeneration 19, 4–6.

Bede, P, Hardiman, O, 2018. Longitudinal structural changes in ALS: a three time-point imaging study of white and gray matter degeneration. Amyotrophic lateral sclerosis & frontotemporal degeneration 19, 232–241.

Bede, P, Iyer, PM, Finegan, E, Omer, T, Hardiman, O, 2017. Virtual brain biopsies in amyotrophic lateral sclerosis: Diagnostic classification based on in vivo pathological patterns. NeuroImage Clinical 15, 653–658.

Bede, P, Iyer, PM, Schuster, C, Elamin, M, McLaughlin, RL, Kenna, K, Hardiman, O, 2016. The selective anatomical vulnerability of ALS: 'disease-defining' and 'disease-defying' brain regions. Amyotrophic lateral sclerosis & frontotemporal degeneration 17, 561–570.

Bede, P, Omer, T, Finegan, E, Chipika, RH, Iyer, PM, Doherty, MA, Vajda, A, Pender, N, McLaughlin, RL, Hutchinson, S, Hardiman, O, 2018. Connectivity-based characterisation of subcortical grey matter pathology in frontotemporal dementia and ALS: a multimodal neuroimaging study. Brain imaging and behavior 12, 1696–1707.

Bede, P, Querin, G, Pradat, PF, 2018. The changing landscape of motor neuron disease imaging: the transition from descriptive studies to precision clinical tools. Curr Opin Neurol 31, 431–438.

Bersano, E, Sarnelli, MF, Solara, V, De Marchi, F, Sacchetti, GM, Stecco, A, Corrado, L, D'alfonso, S, Cantello, R, Mazzini, L, 2018. A case of late-onset OCD developing PLS and FTD. Amyotrophic Lateral Sclerosis and Frontotemporal Degeneration 1–3.

Brettschneider, J, Del Tredici, K, Toledo, JB, Robinson, JL, Irwin, DJ, Grossman, M, Suh, E, Van Deerlin, VM, Wood, EM, Baek, Y, Kwong, L, Lee, EB, Elman, L, McCluskey, L, Fang, L, Feldengut, S, Ludolph, AC, Lee, VM, Braak, H, Trojanowski, JQ, 2013. Stages of pTDP-43 pathology in amyotrophic lateral sclerosis. Annals of neurology 74, 20–38.

Brooks, BR, Miller, RG, Swash, M, Munsat, TL, 2000. World Federation of Neurology Research Group on Motor Neuron D (2000) El Escorial revisited: revised criteria for the diagnosis of amyotrophic lateral sclerosis. Amyotrophic lateral sclerosis and other motor neuron disorders: official publication of the World Federation of Neurology, Research Group on Motor Neuron Diseases 1, 293–299.

Burke, T, Pinto-Grau, M, Lonergan, K, Elamin, M, Bede, P, Costello, E, Hardiman, O, Pender, N, 2016. Measurement of Social Cognition in Amyotrophic Lateral Sclerosis: A Population Based Study. PLoS One 11, e0160850.

Butman, JA, Floeter, MK, 2007. Decreased thickness of primary motor cortex in primary lateral sclerosis. American Journal of Neuroradiology 28, 87–91.

Byrne, S, Elamin, M, Bede, P, Shatunov, A, Walsh, C, Corr, B, Heverin, M, Jordan, N, Kenna, K, Lynch, C, McLaughlin, RL, Iyer, PM, O'Brien, C, Phukan, J, Wynne, B, Bokde, AL, Bradley, DG, Pender, N, Al-Chalabi, A, Hardiman, O, 2012. Cognitive and clinical characteristics of patients with amyotrophic lateral sclerosis carrying a C9orf72 repeat expansion: a population-based cohort study. Lancet neurology 11, 232–240.

Chipika, RH, Finegan, E, Li Hi Shing, S, Hardiman, O, Bede, P, 2019. Tracking a Fast-Moving Disease: Longitudinal Markers, Monitoring, and Clinical Trial Endpoints in ALS. Frontiers in neurology 10, 229.

Christidi, F, Karavasilis, E, Ferentinos, P, Xirou, S, Velonakis, G, Rentzos, M, Zouvelou, V, Zalonis, I, Efstathopoulos, E, Kelekis, N, Evdokimidis, I, 2017. Investigating the neuroanatomical substrate of pathological laughing and crying in amyotrophic lateral sclerosis with multimodal neuroimaging techniques. Amyotroph Lateral Scler Frontotemporal Degener 1–9.

Christidi, F, Karavasilis, E, Ferentinos, P, Xirou, S, Velonakis, G, Rentzos, M, Zouvelou, V, Zalonis, I, Efstathopoulos, E, Kelekis, N, Evdokimidis, I, 2018. Investigating the neuroanatomical substrate of pathological laughing and crying in amyotrophic lateral sclerosis with multimodal neuroimaging techniques. Amyotrophic lateral sclerosis & frontotemporal degeneration 19, 12–20.

Christidi, F, Karavasilis, E, Rentzos, M, Kelekis, N, Evdokimidis, I, Bede, P, 2018. Clinical and Radiological Markers of Extra-Motor Deficits in Amyotrophic Lateral Sclerosis. Frontiers in neurology 9, 1005.

Christidi, F, Karavasilis, E, Rentzos, M, Velonakis, G, Zouvelou, V, Xirou, S, Argyropoulos, G, Papatriantafyllou, I, Pantolewn, V, Ferentinos, P, Kelekis, N, Seimenis, I, Evdokimidis, I, Bede, P, 2019. Hippocampal pathology in Amyotrophic Lateral Sclerosis: selective vulnerability of subfields and their associated projections. Neurobiology of aging.

Christidi, F, Karavasilis, E, Velonakis, G, Ferentinos, P, Rentzos, M, Kelekis, N, Evdokimidis, I, Bede, P, 2018. The Clinical and Radiological Spectrum of Hippocampal Pathology in Amyotrophic Lateral Sclerosis. Frontiers in neurology 9, 523.

Cingolani, P, Platts, A, Wang, LL, Coon, M, Nguyen, T, Wang, L, Land, SJ, Lu, X, Ruden, DM, 2012. A program for annotating and predicting the effects of single nucleotide polymorphisms. SnpEff: SNPs in the genome of Drosophila melanogaster strain w1118; iso-2; iso-3. Fly 6, 80–92.

Clark, M, Huang, C, Bageac, D, Danielian, L, Smallwoed, R, Floeter, MK, 2017. Neuroimaging changes in the first 5 years of symptoms in patients with primary lateral sclerosis. Amyotrophic Lateral Sclerosis and Frontotemporal Degeneration 18, 216–217.

Clark, MG, Smallwood Shoukry, R, Huang, CJ, Danielian, LE, Bageac, D, Floeter, MK, 2018. Loss of functional connectivity is an early imaging marker in primary lateral sclerosis. Amyotrophic lateral sclerosis & frontotemporal degeneration 19, 562–569.

Clinicaltrials.gov (2019) Sinemet for Spasticity and Function in Amyotrophic Lateral Sclerosis and Primary Lateral Sclerosis (ALS and PLS). In, ClincialTrials.gov {Internet}. Bethesda (MD).

de Vries, BS, Rustemeijer, LMM, van der Kooi, AJ, Raaphorst, J, Schröder, CD, Nijboer, TCW, Hendrikse, J, Veldink, JH, van den Berg, LH, van Es, MA, 2017. A case series of PLS patients with frontotemporal dementia and overview of the literature. Amyotrophic Lateral Sclerosis and Frontotemporal Degeneration 18, 534–548.

de Vries, BS, Spreij, LA, Rustemeijer, LMM, Bakker, LA, Veldink, JH, van den Berg, LH, Nijboer, TCW, van Es, MA, 2019. A neuropsychological and behavioral study of PLS. Amyotrophic lateral sclerosis & frontotemporal degeneration 20, 376–384.

Desikan, RS, Segonne, F, Fischl, B, Quinn, BT, Dickerson, BC, Blacker, D, Buckner, RL, Dale, AM, Maguire, RP, Hyman, BT, Albert, MS, Killiany, RJ, 2006. An automated labeling system for subdividing the human cerebral cortex on MRI scans into gyral based regions of interest. NeuroImage 31, 968–980.

Elamin, M, Bede, P, Byrne, S, Jordan, N, Gallagher, L, Wynne, B, O'Brien, C, Phukan, J, Lynch, C, Pender, N, Hardiman, O, 2013. Cognitive changes predict functional decline in ALS: a population-based longitudinal study. Neurology 80, 1590–1597.

Elamin, M, Phukan, J, Bede, P, Jordan, N, Byrne, S, Pender, N, Hardiman, O, 2011. Executive dysfunction is a negative prognostic indicator in patients with ALS without dementia. Neurology 76, 1263–1269.

Elamin, M, Pinto-Grau, M, Burke, T, Bede, P, Rooney, J, O'Sullivan, M, Lonergan, K, Kirby, E, Quinlan, E, Breen, N, Vajda, A, Heverin, M, Pender, N, Hardiman, O, 2017. Identifying behavioural changes in ALS: Validation of the Beaumont Behavioural Inventory (BBI). Amyotrophic lateral sclerosis & frontotemporal degeneration 18, 68–73.

Feron, M, Couillandre, A, Mseddi, E, Termoz, N, Abidi, M, Bardinet, E, Delgadillo, D, Lenglet, T, Querin, G, Welter, ML, Le Forestier, N, Salachas, F, Bruneteau, G, Del Mar Amador, M, Debs, R, Lacomblez, L, Meininger, V, Pelegrini-Issac, M, Bede, P, Pradat, PF, de Marco, G, 2018. Extrapyramidal deficits in ALS: a combined biomechanical and neuroimaging study. Journal of neurology.

Finegan, E, Chipika, RH, Li Hi Shing, S, Doherty, MA, Hengeveld, JC, Vajda, A, Donaghy, C, McLaughlin, RL, Pender, N, Hardiman, O, Bede, P, 2019. The clinical and radiological profile of primary lateral sclerosis: a population-based study. Journal of neurology.

Finegan, E, Chipika, RH, Li Hi Shing, S, Hardiman, O, Bede, P, 2019. Pathological Crying and Laughing in Motor Neuron Disease: Pathobiology, Screening, Intervention. Frontiers in neurology 10, 260.

Finegan, E, Chipika, RH, Shing, SLH, Hardiman, O, Bede, P, 2019. Primary lateral sclerosis: a distinct entity or part of the ALS spectrum? Amyotrophic lateral sclerosis & frontotemporal degeneration 1–13.

Fischl, B, 2012. FreeSurfer. NeuroImage 62, 774–781.

Floeter, MK, Katipally, R, Kim, MP, Schanz, O, Stephen, M, Danielian, L, Wu, T, Huey, ED, Meoded, A, 2014. Impaired corticopontocerebellar tracts underlie pseudobulbar affect in motor neuron disorders. Neurology 83, 620–627.

Floeter, MK, Mills, R, 2009. Progression in primary lateral sclerosis: a prospective analysis. Amyotrophic Lateral Sclerosis 10, 339–346.

Frazier, JA, Chiu, S, Breeze, JL, Makris, N, Lange, N, Kennedy, DN, Herbert, MR, Bent, EK, Koneru, VK, Dieterich, ME, Hodge, SM, Rauch, SL, Grant, PE, Cohen, BM, Seidman, LJ, Caviness, VS, Biederman, J, 2005. Structural brain magnetic resonance imaging of limbic and thalamic volumes in pediatric bipolar disorder. Am J Psychiatry 162, 1256–1265.

Fu, YJ, Tan, CF, Nishihira, Y, Takahashi, H, 2010. Pathological TDP-43 in a case of primary lateral sclerosis. Dementia and Geriatric Cognitive Disorders 30, 37.

Geser, F, Prvulovic, D, O'Dwyer, L, Hardiman, O, Bede, P, Bokde, AL, Trojanowski, JQ, Hampel, H, 2011. On the development of markers for pathological TDP-43 in amyotrophic lateral sclerosis with and without dementia. Progress in neurobiology 95, 649–662.

Ghaffar, O, Chamelian, L, Feinstein, A, 2008. Neuroanatomy of pseudobulbar affect: a quantitative MRI study in multiple sclerosis. Journal of neurology 255, 406–412.

Gordon, P, Cheng, B, Katz, I, Pinto, M, Hays, A, Mitsumoto, H, Rowland, L, 2006. The natural history of primary lateral sclerosis. Neurology 66, 647–653.

Gordon, PH, Cheng, B, Katz, IB, Pinto, M, Hays, AP, Mitsumoto, H, Rowland, LP, 2006. The natural history of primary lateral sclerosis. Neurology 66, 647–653.

Grollemund, V, Pradat, PF, Querin, G, Delbot, F, Le Chat, G, Pradat-Peyre, JF, Bede, P, 2019. Machine Learning in Amyotrophic Lateral Sclerosis: Achievements, Pitfalls, and Future Directions. Frontiers in neuroscience 13, 135.

Hirsch-Reinshagen, V, Alfaify, OA, Hsiung, GYR, Pottier, C, Baker, M, Perkerson, RB, Rademakers, R, Briemberg, H, Foti, DJ, Mackenzie, IR, 2019. Clinicopathologic correlations in a family with a TBK1 mutation presenting as primary progressive aphasia and primary lateral sclerosis. Amyotrophic Lateral Sclerosis and Frontotemporal Degeneration.

Iglesias, JE, Augustinack, JC, Nguyen, K, Player, CM, Player, A, Wright, M, Roy, N, Frosch, MP, McKee, AC, Wald, LL, Fischl, B, Van Leemput, K, 2015. A computational atlas of the hippocampal formation using ex vivo, ultra-high resolution MRI: Application to adaptive segmentation of in vivo MRI. NeuroImage 115, 117–137.

Iwata, NK, Kwan, JY, Danielian, LE, Butman, JA, Tovar-Moll, F, Bayat, E, Floeter, MK, 2011. White matter alterations differ in primary lateral sclerosis and amyotrophic lateral sclerosis. Brain: a journal of neurology 134, 2642–2655.

Jenkinson, M, Smith, S, 2001. A global optimisation method for robust affine registration of brain images. Medical image analysis 5, 143–156.

Kassubek, J, Muller, HP, Del Tredici, K, Brettschneider, J, Pinkhardt, EH, Lule, D, Bohm, S, Braak, H, Ludolph, AC, 2014. Diffusion tensor imaging analysis of sequential spreading of disease in amyotrophic lateral sclerosis confirms patterns of TDP-43 pathology. Brain: a journal of neurology 137, 1733–1740.

Kenna, KP, McLaughlin, RL, Byrne, S, Elamin, M, Heverin, M, Kenny, EM, Cormican, P, Morris, DW, Donaghy, CG, Bradley, DG, Hardiman, O, 2013. Delineating the genetic heterogeneity of ALS using targeted high-throughput sequencing. J Med Genet 50, 776–783.

Klebe, S, Stevanin, G, Depienne, C, 2015. Clinical and genetic heterogeneity in hereditary spastic paraplegias: from SPG1 to SPG72 and still counting. Rev Neurol (Paris) 171, 505–530.

Kosaka, T, Fu, YJ, Shiga, A, Ishidaira, H, Tan, CF, Tani, T, Koike, R, Onodera, O, Nishizawa, M, Kakita, A, Takahashi, H, 2012. Primary lateral sclerosis: upper-motor-predominant amyotrophic lateral sclerosis with frontotemporal lobar degeneration–immunohistochemical and biochemical analyses of TDP-43. Neuropathology: official journal of the Japanese Society of Neuropathology 32, 373–384.

Li H, Handsaker B, Wysoker A, Fennell T, Ruan J, Homer N, Marth G, Abecasis G, Durbin R, Genome Project Data Processing S (2009) The Sequence Alignment/Map format and SAMtools. Bioinformatics (Oxford, England) 25:2078-2079.

Mabuchi, N, Watanabe, H, Atsuta, N, Hirayama, M, Ito, H, Fukatsu, H, Kato, T, Ito, K, Sobue, G, 2004. Primary lateral sclerosis presenting parkinsonian symptoms without nigrostriatal involvement. Journal of Neurology. Neurosurgery and Psychiatry 75, 1768–1771.

Machts, J, Loewe, K, Kaufmann, J, Jakubiczka, S, Abdulla, S, Petri, S, Dengler, R, Heinze, HJ, Vielhaber, S, Schoenfeld, MA, Bede, P, 2015. Basal ganglia pathology in ALS is associated with neuropsychological deficits. Neurology 85, 1301–1309.

Martin M (2011) Cutadapt removes adapter sequences from high-throughput sequencing reads. EMBnetjournal.

McLaughlin, RL, Kenna, KP, Vajda, A, Bede, P, Elamin, M, Cronin, S, Donaghy, CG, Bradley, DG, Hardiman, O, 2015. Second-generation Irish genome-wide association study for amyotrophic lateral sclerosis. Neurobiology of aging 36 1221.e1227-1213.

Müller, HP, Gorges, M, Kassubek, R, Dorst, J, Ludolph, AC, Kassubek, J, 2018. Identical patterns of cortico-efferent tract involvement in primary lateral sclerosis and amyotrophic lateral sclerosis: A tract of interest-based MRI study. NeuroImage: Clinical 18, 762–769.

Nichols, TE, Holmes, AP, 2002. Nonparametric permutation tests for functional neuroimaging: a primer with examples. Hum Brain Mapp 15, 1–25.

Olney, RK, Murphy, J, Forshew, D, Garwood, E, Miller, BL, Langmore, S, Kohn, MA, Lomen-Hoerth, C, 2005. The effects of executive and behavioral dysfunction on the course of ALS. Neurology 65, 1774–1777.

Omer, T, Finegan, E, Hutchinson, S, Doherty, M, Vajda, A, McLaughlin, RL, Pender, N, Hardiman, O, Bede, P, 2017. Neuroimaging patterns along the ALS-FTD spectrum: a multiparametric imaging study. Amyotrophic lateral sclerosis & frontotemporal degeneration 1–13.

Paila, U, Chapman, BA, Kirchner, R, Quinlan, AR, 2013. GEMINI: integrative exploration of genetic variation and genome annotations. PLoS computational biology 9, e1003153.

Patenaude, B, Smith, SM, Kennedy, DN, Jenkinson, M, 2011. A Bayesian model of shape and appearance for subcortical brain segmentation. NeuroImage 56, 907–922.

Phukan, J, Elamin, M, Bede, P, Jordan, N, Gallagher, L, Byrne, S, Lynch, C, Pender, N, Hardiman, O, 2012. The syndrome of cognitive impairment in amyotrophic lateral sclerosis: a population-based study. Journal of neurology, neurosurgery, and psychiatry 83, 102–108.

Project Min, EALSSC, 2018. Project MinE: study design and pilot analyses of a large-scale whole-genome sequencing study in amyotrophic lateral sclerosis. European journal of human genetics: EJHG 26, 1537–1546.

Purcell, S, Neale, B, Todd-Brown, K, Thomas, L, Ferreira, MAR, Bender, D, Maller, J, Sklar, P, de Bakker, PIW, Daly, MJ, Sham, PC, 2007. PLINK: a tool set for whole-genome association and population-based linkage analyses. American journal of human genetics 81, 559–575.

Querin, G, El Mendili, MM, Bede, P, Delphine, S, Lenglet, T, Marchand-Pauvert, V, Pradat, PF, 2018. Multimodal spinal cord MRI offers accurate diagnostic classification in ALS. Journal of neurology, neurosurgery, and psychiatry.

Rascovsky, K, Hodges, JR, Knopman, D, Mendez, MF, Kramer, JH, Neuhaus, J, van Swieten, JC, Seelaar, H, Dopper, EGP, Onyike, CU, Hillis, AE, Josephs, KA, Boeve, BF, Kertesz, A, Seeley, WW, Rankin, KP, Johnson, JK, Gorno-Tempini, ML, Rosen, H, Prioleau-Latham, CE, Lee, A, Kipps, CM, Lillo, P, Piguet, O, Rohrer, JD, Rossor, MN, Warren, JD, Fox, NC, Galasko, D, Salmon, DP, Black, SE, Mesulam, M, Weintraub, S, Dickerson, BC, Diehl-Schmid, J, Pasquier, F, Deramecourt, V, Lebert, F, Pijnenburg, Y, Chow, TW, Manes, F, Grafman, J, Cappa, SF, Freedman, M, Grossman, M, Miller, BL, 2011. Sensitivity of revised diagnostic criteria for the behavioural variant of frontotemporal dementia. Brain: a journal of neurology 134, 2456–2477.

Rowland, LP, 2005. Primary lateral sclerosis, hereditary spastic paraplegia, and mutations in the alsin gene: historical background for the first International Conference. Amyotrophic lateral sclerosis and other motor neuron disorders: official publication of the World Federation of Neurology. Research Group on Motor Neuron Diseases 6, 67–76.

Schuster, C, Elamin, M, Hardiman, O, Bede, P, 2015. Presymptomatic and longitudinal neuroimaging in neurodegeneration–from snapshots to motion picture: a systematic review. Journal of neurology, neurosurgery, and psychiatry 86, 1089–1096.

Schuster, C, Elamin, M, Hardiman, O, Bede, P, 2016. The segmental diffusivity profile of amyotrophic lateral sclerosis associated white matter degeneration. Eur J Neurol 23, 1361–1371.

Schuster, C, Hardiman, O, Bede, P, 2016. Development of an Automated MRI-Based Diagnostic Protocol for Amyotrophic Lateral Sclerosis Using Disease-Specific Pathognomonic Features: A Quantitative Disease-State Classification Study. PLoS One 11, e0167331.

Schuster, C, Hardiman, O, Bede, P, 2017. Survival prediction in Amyotrophic lateral sclerosis based on MRI measures and clinical characteristics. BMC Neurol 17, 73.

Schuster, C, Kasper, E, Machts, J, Bittner, D, Kaufmann, J, Benecke, R, Teipel, S, Vielhaber, S, Prudlo, J, 2013. Focal thinning of the motor cortex mirrors clinical features of amyotrophic lateral sclerosis and their phenotypes: a neuroimaging study. Journal of neurology 260, 2856–2864.

Smith, SM, Nichols, TE, 2009. Threshold-free cluster enhancement: addressing problems of smoothing, threshold dependence and localisation in cluster inference. NeuroImage 44, 83–98.

Sugihara, H, Horiuchi, M, Kamo, T, Fujisawa, K, Abe, M, Sakiyama, T, Tadokoro, M, 1999. A case of primary lateral sclerosis taking a prolonged clinical course with dementia and having an unusual dendritic ballooning. Neuropathology: official journal of the Japanese Society of Neuropathology 19, 77–84.

Thakore, N, Pioro, E, 2014. Prevalence, associations and course of depression in ALS: Observations from a large cohort. Amyotrophic Lateral Sclerosis and Frontotemporal Degeneration 15, 55–56.

Unrath, A, Muller, H-P, Riecker, A, Ludolph, AC, Sperfeld, A-D, Kassubek, J, 2010. Whole brain-based analysis of regional white matter tract alterations in rare motor neuron diseases by diffusion tensor imaging. Hum Brain Mapp 31, 1727–1740.

Van Weehaeghe, D, Ceccarini, J, Delva, A, Robberecht, W, Van Damme, P, Van Laere, K, 2016. Prospective validation of 18 F-FDG brain PET discriminant analysis methods in the diagnosis of amyotrophic lateral sclerosis. Journal of Nuclear Medicine 57, 1238–1243.

Westeneng, HJ, Verstraete, E, Walhout, R, Schmidt, R, Hendrikse, J, Veldink, JH, van den Heuvel, MP, van den Berg, LH, 2015. Subcortical structures in amyotrophic lateral sclerosis. Neurobiology of aging 36, 1075–1082.

Winkler, AM, Ridgway, GR, Webster, MA, Smith, SM, Nichols, TE, 2014. Permutation inference for the general linear model. NeuroImage 92, 381–397.

Woo, JH, Wang, S, Melhem, ER, Gee, JC, Cucchiara, A, McCluskey, L, Elman, L, 2014. Linear associations between clinically assessed upper motor neuron disease and diffusion tensor imaging metrics in amyotrophic lateral sclerosis. PLoS ONE [Electronic Resource] 9, e105753.

Yunusova, Y, Plowman, EK, Green, JR, Barnett, C, Bede, P, 2019. Clinical Measures of Bulbar Dysfunction in ALS. Frontiers in neurology 10, 106.

Zhang, Y, Brady, M, Smith, S, 2001. Segmentation of brain MR images through a hidden Markov random field model and the expectation-maximization algorithm. IEEE transactions on medical imaging 20, 45–57.